Investigation on Gaussian Waveforms to Improve Robustness in Physical Layer Network Coding

Stephan Schedler, and Volker Kühn
University of Rostock, Rostock, Germany
Email: {stephan.schedler, volker.kuehn}@uni-rostock.de

Matthias Woltering, Dirk Wübben, and Armin Dekorsy
University of Bremen, Bremen, Germany
Email: {woltering, wuebben, dekorsy}@ant.uni-bremen.de

***Abstract*— In this paper, two-way relaying networks using physical layer network coding under practical constraints are considered. In the multiple access phase, both users transmit their messages simultaneously on the same resources. At the relay a superposition of both massages is received containing the influence of the channel as well as the impact of Carrier Frequency Offsets (CFOs) and Timing Offsets (TOs), respectively. To be more robust against these impacts, a combination of a generalized Frequency Division Multiplexing (FDM) system, which uses Gaussian waveforms is analyzed in comparison to classical Orthogonal Frequency Division Multiplexing (OFDM). The additional interference introduced by the non-orthogonal impulse shape is treated by an additional linear equalizer. The overall system performance of the classical OFDM system and non-orthogonal waveforms is compared for Physical-Layer Network Coding (PLNC) with respect to the Signal to Interference and Noise Ratio (SINR) and the achievable mutual information in the PLNC system. The obtained simulation results show that a well designed Gaussian waveform outperforms the classical OFDM system with guard interval.**

***Index Terms*— synchronization offsets, generalized FDM, linear MMSE equalizer, Physical-Layer Network Coding (PLNC), Two Way Relay Channel (TWRC).**

I. Introduction

In a Two Way Relay Channel (TWRC) the spectral efficiency can be improved significantly by Physical-Layer Network Coding (PLNC), where the data of two users is transmitted to an assisting relay in a Multiple Access Channel (MAC) phase, and the network coded signal is broadcasted by the relay in a second time slot (broadcast phase) [1], [2]. As the user terminals are aware of their own messages, they can extract the message of the other user from the received relay message. The superposition of the two messages at the relay contains inherent interference due to the influence of the channel as well as impairments like CFO and TO, even if an orthogonal system is used. Since OFDM is widely used in current mobile transmission standards, the combination of OFDM and PLNC has been proposed in [3]–[7]. However, OFDM has some considerable drawbacks like high out-of-band radiation, sensitivity to CFOs and high Peak to Average Power Ratio (PAPR). Recently much research has been done to improve the robustness of multicarrier systems regarding these effects. In [8] subcarrier-wise filtering is considered named Offset-QAM/Filter Bank Multi-Carrier (OQAM/FBMC). Here, well-localized filters can be used to generate an orthogonal transmit scheme. Another scheme is Universal Filtered Multicarrier (UFMC), which is a subblock-based filtered OFDM system introduced in [9]. More general schemes, which introduce non-orthogonal multicarrier transmission are given in [10], [11]. In thesis [10] a general view on generalized FDM is given, whereas the paper [11] deals with a block-based realization, similar to OFDM. An overview of non-orthogonal waveforms in mobile applications is given in [12].

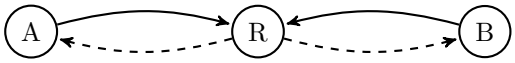

Fig. 1: A TWRC with MAC phase (solid lines) and BC phase (dashed lines).

In general, different names are given for the similar schemes in literature. In most cases Filter Bank Multi-Carrier (FBMC) refers to OQAM/FBMC or OQAM/OFDM, but the term FBMC might also be used more general. The authors in [10], [11] use the term GFDM, but the meaning is different. Similar to the work of Du [10], we will use Generalized FDM (GFDM) as a term for a general multicarrier scheme with non-orthogonal transmit filters. Contrary to OFDM that is based on orthogonal rectangular filters, GFDM systems can also utilize non-orthogonal waveforms to enable more flexible spectrum shaping. By this means, the spectral efficiency, the influence of doubly dispersive channels, or sensitivity to synchronization offsets can be improved as shown in [13]. Nevertheless, this comes at the cost of additional interference and increased computational complexity.

A common example is the application of a Gaussian prototype filter. Even if it does not satisfy the first Nyquist criterion, the interference is mainly limited to neighboring symbols in the time frequency grid as it decays fast. Furthermore, the Gaussian impulse has the same shape in time and frequency and it is optimally concentrated [8], [14]. Compared to an orthogonal scheme, however, equalization is more complex.

Due to these properties, we propose a combination of GFDM and PLNC to be more robust against channel influence and practical impairments. Within this paper, we will investigate the robustness of Gaussian prototype filters in a PLNC system. The Inter-Symbol Interference (ISI) and Inter-Carrier Interference (ICI) that is caused by the non-orthogonal design is treated by a Minimum Mean Square Error (MMSE) equalizer. We will show

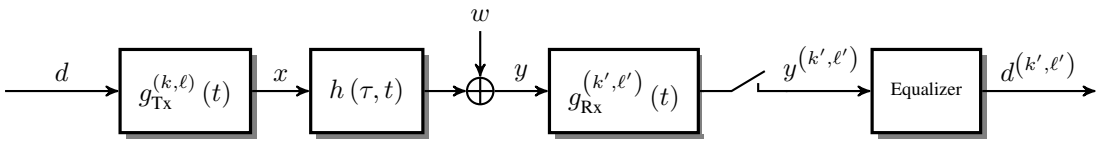

Fig. 2: Block diagram of a P2P link for a GFDM system with equalizer.

that the application of Gaussian waveform and subsequent equalizer leads to a system that is less sensitive to synchronization errors than OFDM. To evaluate the overall system performance we will provide simulation results for a PLNC system.

The paper is organized as follows. In Sec. II, a recapitulation of the GFDM system model is given for a P2P system. Sec. III extends the system model to a PLNC scheme in a TWRC. Afterwards, Sec. IV introduces Signal to Interference and Noise Ratio (SINR) and mutual information that are used to evaluate the system performance. Finally, Sec. V shows some numerical results and Sec. VI concludes the paper.

Notations: In this paper, lower case bold characters are used to denote vectors, upper case bold characters denote matrices. $(\cdot)^T$ denotes the transpose of a vector, $(\cdot)^*$ is the conjugate complex, $\Pr(\cdot)$ denotes some probability and $p(\cdot)$ is a Probability Density Function (PDF).

II. GFDM FOR P2P (RECAP)

Within this section we provide a short recapitulation of the GFDM system model for a P2P link as depicted in Fig. 2. Later, this system model will be extended for the TWRC. We assume that transmitter and receiver are equipped with a single antenna and the transmission is done on several subcarriers k in successive time slots ℓ.

A. System Model

The transmit signal $x(t)$ at the transmitter is given by

$$x(t) = \sum_k \sum_\ell d^{(k,\ell)} g_{\text{Tx}}^{(k,\ell)}(t) \quad , \tag{1}$$

where $d^{(k,\ell)}$ is the transmit symbol on the kth subcarrier in the ℓth time slot, and $g_{\text{Tx}}^{(k,\ell)}(t)$ is the transmit filter $g_{\text{Tx}}(t)$ shifted to lattice point (k,ℓ)

$$g_{\text{Tx}}^{(k,\ell)}(t) = g(t-\ell T)\, e^{j2\pi(kF)t} \quad . \tag{2}$$

In general, a lattice point (k,ℓ) defines the position of the modulated pulse in the time-frequency grid as well as the sampling position at the receiver. The lattice points of a rectangular grid are visualized in Fig. 3, where the data symbols are transmitted on frequency carrier k during time slot ℓ. The spectral efficiency $\beta/(TF)$ of the system can be defined by subcarrier spacing F and symbol length T, with β bits per symbol.

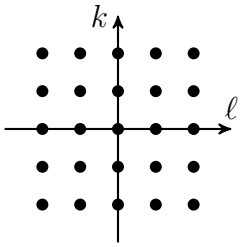

Fig. 3: Rectangular lattice grid in time-frequency plane with subcarriers k and time slots ℓ.

After passing channel $h(\tau,t)$ the received signal is given by [10]

$$y(t) = \int h(\tau,t)\, x(t-\tau)\, d\tau + w(t) \tag{3}$$

$$= \sum_k \sum_\ell d^{(k,\ell)} \iint H(\tau,\nu)\, g_{\text{Tx}}^{(k,\ell)}(t-\tau) \cdot e^{j2\pi t\nu} d\nu d\tau + w(t)\,, \tag{4}$$

where $h(\tau,t)$, $H(\tau,\nu)$ and $w(t)$ denote the time-variant channel impulse response, the Delay-Doppler function and Additive White Gaussian Noise (AWGN) with $w \sim \mathcal{CN}(0,\sigma_W^2)$.

According to the matched filter condition $g_{\text{Rx}}(t) = g_{\text{Tx}}^*(-t)$, the receive filter is given by

$$g_{\text{Rx}}^{(k',\ell')}(t) = g^*(-t-\ell' T-\Delta\tau) \cdot e^{-j2\pi\left(k'F+\Delta\nu\right)(-t)} \quad , \tag{5}$$

where the position of the receive filter in the time-frequency grid is defined by lattice point (k',ℓ'). The CFO $\Delta\nu$ and TO $\Delta\tau$ lead to additional shifts of the receive filter in time or frequency such that the optimal sampling position cannot be met. If the receiver of the P2P system is aware of these synchronization offsets, the offsets might be compensated by shifting the sampling position in the time-frequency grid. Note that this will not be possible in the TWRC that is considered later. Due to the superposition of signal in the MAC phase of a PLNC system, the relay cannot compensate the offsets to both users even if it would be aware of them [15].

After sampling at position $t=0$, we obtain the received P2P symbol

$$y^{(k',\ell')} = \int_{-\infty}^{+\infty} y(\lambda)\, g_{\text{Rx}}^{(k',\ell')}(t-\lambda) d\lambda \Big|_{t=0} \quad . \tag{6}$$

$$y^{(k',\ell')} = \sum_k \sum_\ell d^{(k,\ell)} \iint H(\tau,\nu)\, e^{-2j\pi\left((kF)\tau+\left(F\left(k'-k\right)+\Delta\nu-\nu\right)\left(\frac{1}{2}\left((\ell'+\ell)T+\Delta\tau+\tau\right)\right)\right)}$$

$$\cdot A^*\left(T\left(\ell-\ell'\right)-\Delta\tau+\tau, F\left(k-k'\right)-\Delta\nu+\nu\right) d\nu d\tau + \int_{-\infty}^{+\infty} w^*(\lambda)\, g_{\text{Rx}}^{(k',\ell')}(-\lambda)\, d\lambda \qquad (7)$$

By inserting (4), (5) into (6) we obtain (7), where $A(\tau,\nu)$ is the ambiguity function

$$A(\tau,\nu) = \int g^*\left(t+\frac{\tau}{2}\right) g\left(t-\frac{\tau}{2}\right) e^{j2\pi\nu t} dt \quad . \qquad (8)$$

Equation (7) is similar to the result in [13], but it takes synchronization offsets into account. Analytical expressions of the ambiguity functions are given in [10] for several pulse shapes. For a multi-path channel with statistically independent paths, the Delay-Doppler function $H(\tau,\nu)$ is given by a summation over time and frequency shifted Dirac functions. Thus, the double integral in (7)

$$\vartheta^{(k,\ell,k',\ell')} = \iint H(\tau,\nu)\, e^{-2j\pi(\cdots)} A^*(\cdots)\, d\nu d\tau \qquad (9)$$

can be solved analytically for specific transmit filters. For ease of notation, the double integral is substituted by coefficient $\vartheta^{(k,\ell,k',\ell')}$. Then the received symbol is given by

$$y^{(k',\ell')} = \sum_k \sum_\ell d^{(k,\ell)} \vartheta^{(k,\ell,k',\ell')} + \widetilde{w} \qquad (10)$$

with $\widetilde{w}$ as filtered noise term. The summations in (10) need to be done over all lattice points (k,ℓ) that might have an influence on the received symbol at (k',ℓ'). Note that the coefficients $\vartheta^{(k,\ell,k',\ell')}$ depend on the utilized waveform, the instantaneous channel, the considered lattice points, as well as synchronization offsets $\Delta\nu$ and $\Delta\tau$.

B. Matrix Representation

Next, we will introduce an alternative notation for received symbol $y^{(k',\ell')}$ that will be used to compute equalizer coefficients. We will use an approximation that only considers the influence of N_d neighboring transmit symbols

$$y^{(k',\ell')} \approx \boldsymbol{\vartheta}^{(k',\ell')\text{T}} \boldsymbol{d}^{(k',\ell')} + \widetilde{w} \quad , \qquad (11)$$

where $\boldsymbol{\vartheta}^{(k',\ell')}$ is a stacked vector of N_d channel coefficients that describe the influence of N_d transmit symbols on received symbol $y^{(k',\ell')}$. Vector $\boldsymbol{d}^{(k',\ell')}$ consists of the N_d corresponding transmit symbols. Interference that is caused by lattice points that are not stacked in $\boldsymbol{\vartheta}^{(k',\ell')}$ is ignored. Fig. 4 depicts an example for $\boldsymbol{\vartheta}^{(0,0)}$ and $N_\text{d} = 49$ neighboring lattice points. The outer rectangular area covers the $N_\text{d} = 49$ neighboring lattice points whose coefficients are stacked in vector $\boldsymbol{\vartheta}^{(0,0)}$. Note that (11) is an approximation of the received symbol $y^{(k',\ell')}$ that is only tight if N_d is chosen appropriately large and all the significant interference terms from neighboring lattice points are considered. For the sake of simplicity, the superscript in vectors $\boldsymbol{\vartheta}^{(k',\ell')}$ and $\boldsymbol{d}^{(k',\ell')}$ will be omitted subsequently.

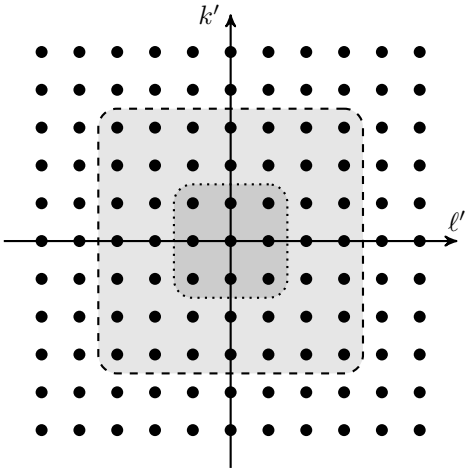

Fig. 4: Visualization of the time-frequency grid around lattice point $(k',\ell') = (0,0)$. The inner area covers the $N_\text{y} = 9$ received symbols in $\boldsymbol{y}$. The outer rectangle covers the $N_\text{d} = 49$ neighboring symbols in $\boldsymbol{d}$ whose influence is still considered at the $N_\text{y} = 9$ received symbols.

With above definitions we can also define vector $\boldsymbol{y}^{(k',\ell')}$ that stacks the N_y adjacent received symbols around lattice point (k',ℓ'), i.e.

$$\boldsymbol{y}^{(k',\ell')} \approx \boldsymbol{V} \cdot \boldsymbol{d} + \boldsymbol{w} \quad . \qquad (12)$$

Matrix $\boldsymbol{V}$ contains the coefficients of the links from the N_d transmit symbols towards the N_y received symbols. Thus, $\boldsymbol{V}$ is of size $N_\text{y} \times N_\text{d}$. Vector $\boldsymbol{w}$ consists of the noise terms that correspond to the N_y received signals. Fig. 4 visualizes an example for $\boldsymbol{y}^{(0,0)}$ and $N_\text{y} = 9$, where the inner rectangle covers the $N_\text{y} = 9$ received symbols around lattice point $(0,0)$. A specific example of (12) for $N_\text{d} = 9$, $N_\text{y} = 9$, and $(k',\ell') = (0,0)$ is given in (13) and (14).

Finally, we can define equalizer $\boldsymbol{z}^T$ that estimates symbol (k',ℓ') based upon the N_y received symbols.

$$y_\text{Eq}^{(k',\ell')} = \boldsymbol{z}^T \boldsymbol{y}^{(k',\ell')} \quad . \qquad (15)$$

The equalizer coefficients stacked in vector $\boldsymbol{z}^T$ will be denoted $z^{(k,\ell,k',\ell')}$. Inserting (12) in (15) we can also find a matrix representation that incorporates channel, waveform and equalizer

$$y_\text{Eq}^{(k',\ell')} = \boldsymbol{\vartheta}_\text{Eq}^\text{T} \cdot \boldsymbol{d} + \boldsymbol{z}^T \boldsymbol{w} \quad , \qquad (16)$$

where vector $\boldsymbol{\vartheta}_\text{Eq}^\text{T} = \boldsymbol{z}^T \boldsymbol{V}$ consists of elements $\vartheta_\text{Eq}^{(k,\ell,k',\ell')}$.

$$\begin{bmatrix} \begin{bmatrix} y^{(-1,-1)} \\ y^{(-1,\pm 0)} \\ y^{(-1,+1)} \end{bmatrix} \\ \begin{bmatrix} y^{(\pm 0,-1)} \\ y^{(\pm 0,\pm 0)} \\ y^{(\pm 0,+1)} \end{bmatrix} \\ \begin{bmatrix} y^{(+1,-1)} \\ y^{(+1,\pm 0)} \\ y^{(+1,+1)} \end{bmatrix} \end{bmatrix} = \begin{bmatrix} \tilde{\boldsymbol{V}}^{(-1,-1)} & \tilde{\boldsymbol{V}}^{(-1,\pm 0)} & \tilde{\boldsymbol{V}}^{(-1,+1)} \\ \tilde{\boldsymbol{V}}^{(\pm 0,-1)} & \tilde{\boldsymbol{V}}^{(\pm 0,\pm 0)} & \tilde{\boldsymbol{V}}^{(\pm 0,+1)} \\ \tilde{\boldsymbol{V}}^{(+1,-1)} & \tilde{\boldsymbol{V}}^{(+1,\pm 0)} & \tilde{\boldsymbol{V}}^{(+1,+1)} \end{bmatrix} \cdot \begin{bmatrix} \begin{bmatrix} d^{(-1,-1)} \\ d^{(-1,\pm 0)} \\ d^{(-1,+1)} \end{bmatrix} \\ \begin{bmatrix} d^{(\pm 0,-1)} \\ d^{(\pm 0,\pm 0)} \\ d^{(\pm 0,+1)} \end{bmatrix} \\ \begin{bmatrix} d^{(+1,-1)} \\ d^{(+1,\pm 0)} \\ d^{(+1,+1)} \end{bmatrix} \end{bmatrix} + \begin{bmatrix} \begin{bmatrix} w^{(-1,-1)} \\ w^{(-1,\pm 0)} \\ w^{(-1,+1)} \end{bmatrix} \\ \begin{bmatrix} w^{(\pm 0,-1)} \\ w^{(\pm 0,\pm 0)} \\ w^{(\pm 0,+1)} \end{bmatrix} \\ \begin{bmatrix} w^{(+1,-1)} \\ w^{(+1,\pm 0)} \\ w^{(+1,+1)} \end{bmatrix} \end{bmatrix} \tag{13}$$

$$\tilde{\boldsymbol{V}}^{(\kappa',\kappa)} = \begin{bmatrix} \vartheta^{(\kappa,-1,\kappa',-1)} & \vartheta^{(\kappa,\pm 0,\kappa',-1)} & \vartheta^{(\kappa,+1,\kappa',-1)} \\ \vartheta^{(\kappa,-1,\kappa',\pm 0)} & \vartheta^{(\kappa,\pm 0,\kappa',\pm 0)} & \vartheta^{(\kappa,+1,\kappa',\pm 0)} \\ \vartheta^{(\kappa,-1,\kappa',+1)} & \vartheta^{(\kappa,\pm 0,\kappa',+1)} & \vartheta^{(\kappa,+1,\kappa',+1)} \end{bmatrix} \tag{14}$$

C. Waveforms

Within this paper two different schemes will be compared, a classical Cyclic Prefix (CP)-OFDM scheme, and a generalized scheme with Gaussian prototype filter [10]. The transmit and receive filters for the rectangular waveform with a guard interval in CP-OFDM are given by

$$g_{\text{Tx}}(t) = \begin{cases} \frac{1}{\sqrt{T}} & \text{for } |t| \leq \frac{T}{2} \\ 0 & \text{else} \end{cases} \tag{17}$$

$$g_{\text{Rx}}(t) = \begin{cases} \frac{1}{\sqrt{T}} & \text{for } |t| \leq \frac{T-T_{\text{G}}}{2} \\ 0 & \text{else} \end{cases}, \tag{18}$$

where T_{G} is the duration of the guard interval. In case of a perfectly synchronized OFDM system ($\Delta\nu = 0$, $\Delta\tau = 0$), the coefficients become $\vartheta = 1$ for the desired signal part and $\vartheta = 0$ for all interference terms.

If non-orthogonal waveforms are applied or if the channel is dispersive in time or frequency, there might be ICI as well as ISI. Within this paper we will consider a Gaussian impulse shape [14]

$$g_{\text{Tx}}(t) = g_{\text{Rx}}(t) = (2\alpha)^{\frac{1}{4}} e^{-\pi\alpha t^2}. \tag{19}$$

Note that the Fourier transform of (19) is the Gaussian function again, where parameter α influences the localization in time and frequency domain. For $\alpha = 1$ the Gaussian waveform has identical response in time and frequency. Contrary to the rectangular waveform, the Gaussian function leads to a non-orthogonal system, i.e., the first Nyquist criterion is not fulfilled. Thus, there is always interference from neighboring lattice points even if the system is perfectly synchronized. On the other hand, it is optimally concentrated [14] and most interference is restricted to direct neighbors.

If the system is perfectly synchronized ($\Delta\nu = 0$, $\Delta\tau = 0$), for the Gaussian prototype filter the coefficients become

$$\begin{aligned} \vartheta_{\text{Gaussian}}^{(k,\ell,k',\ell')} =& e^{-\frac{1}{2}\pi\left((k'-k)^2F^2+(\ell'-\ell)^2T^2\right)} \\ & \cdot e^{-j\pi(k'-k)F(\ell'+\ell)T} \end{aligned} \tag{20}$$

III. GFDM FOR TWRC

Next, we will extend the system model according to the TWRC, where two users A and B that are assisted by relay R intend to exchange messages. In a PLNC scheme [16], [17] two phases are required for transmission. First, both users A, B transmit simultaneously to relay node R in the MAC-phase. Second, the relay node forwards a combination of both user signals in the broadcast phase. Afterwards the users are able to remove the original signals from the received relay signal.

Subsequently, we will focus on the MAC phase of the PLNC scheme as this is the critical phase where synchronization offsets might have severe influence. A block diagram of the MAC phase is depicted in Fig. 5. If the second user is ignored, it is equivalent to the P2P system in Fig. 2. As in the P2P system we assume that there are TOs and CFOs between the relay and the users. These synchronization offsets are independent random variables, i.e., the relay has to deal with different offsets towards users A and B. Furthermore, we assume that the relay is unaware of these offsets.

Equivalently to the above definitions for the P2P system, we can define the received symbol at relay R

$$\begin{aligned} y_{\text{R}}^{(k',\ell')} =& \sum_k \sum_\ell d_{\text{A}}^{(k,\ell)} \vartheta_{\text{A}}^{(k,\ell,k',\ell')} + \\ & \sum_k \sum_\ell d_{\text{B}}^{(k,\ell)} \vartheta_{\text{B}}^{(k,\ell,k',\ell')} + \widetilde{w} \quad . \end{aligned} \tag{21}$$

As depicted in Fig. 5, it is the superposition of individual signals from user A and B. If again only the interference from the N_{d} adjacent lattice points is considered, the N_{y}

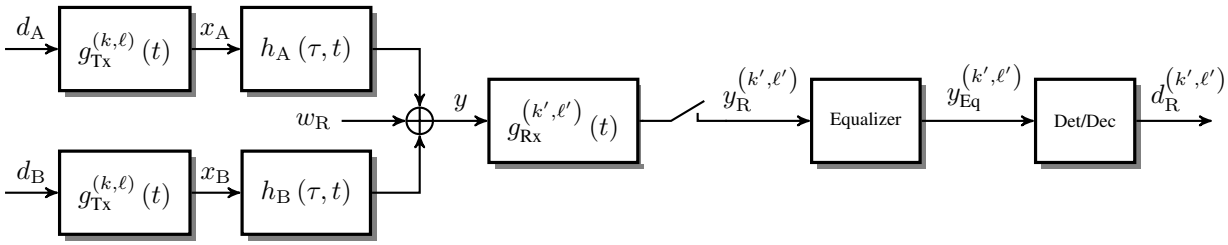

Fig. 5: Block diagram of the MAC phase of a PLNC system with GFDM.

received symbols around (k',ℓ') are given by vector

$$\boldsymbol{y}_{\mathrm{R}}^{(k',\ell')} \approx \boldsymbol{V}_{\mathrm{A}} \cdot \boldsymbol{d}_{\mathrm{A}} + \boldsymbol{V}_{\mathrm{B}} \cdot \boldsymbol{d}_{\mathrm{B}} + \boldsymbol{w} \tag{22}$$

As said above, there is no equalizer $\boldsymbol{z}^T$

$$\begin{aligned} y_{\mathrm{Eq}}^{(k',\ell')} &= \boldsymbol{z}^T \boldsymbol{y}_{\mathrm{R}} \\ &= \boldsymbol{\vartheta}_{\mathrm{Eq,A}}^{\mathrm{T}} \cdot \boldsymbol{d}_{\mathrm{A}} + \boldsymbol{\vartheta}_{\mathrm{Eq,B}}^{\mathrm{T}} \cdot \boldsymbol{d}_{\mathrm{B}} + \boldsymbol{z}^T \boldsymbol{w} \quad , \end{aligned} \tag{23}$$

that eliminates $\boldsymbol{V}_{\mathrm{A}}$ as well as $\boldsymbol{V}_{\mathrm{B}}$ if $\boldsymbol{V}_{\mathrm{A}} \neq \boldsymbol{V}_{\mathrm{B}}$ [15], [18]. Nonetheless, we can compute equalizer coefficients to estimate the superposition of the individual transmit signals. Assuming MMSE criterion, the equalizer coefficients to estimate

$$\tilde{d}_{\mathrm{R}}^{(k',\ell')} = d_{\mathrm{A}}^{(k',\ell')} + d_{\mathrm{B}}^{(k',\ell')} e^{j2\pi\phi} \tag{24}$$

are determined by solving the optimization problem

$$\boldsymbol{z}_{\mathrm{MMSE}}^T = \underset{\boldsymbol{z}^T}{\operatorname{argmin}}\, \mathrm{E}\left\{ \left| y_{\mathrm{Eq}}^{(k',\ell')} - \tilde{d}_{\mathrm{R}}^{(k',\ell')} \right|^2 \right\} \quad . \tag{25}$$

The optimal choice of phase difference ϕ is not obvious but out of the scope of this paper. It depends on the transmit power, the actual modulation scheme, and the used detection scheme at the relay [19]. To simplify matters, we will assume phase difference $\phi = 0$ as in [20]. Then the solution of problem (25) is given by [20]

$$\boldsymbol{z}_{\mathrm{MMSE}}^T = (\boldsymbol{V}_A^H + \boldsymbol{V}_B^H) \left(\boldsymbol{V}_A \, \boldsymbol{V}_A^H + \boldsymbol{V}_B \, \boldsymbol{V}_B^H + \frac{\sigma_W^2}{\sigma_S^2} \, I \right)^{-1} \cdot \mathbf{1} \, , \tag{26}$$

where vector $\mathbf{1} = [0, \cdots, 0, 1, 0, \cdots, 0]^T$ selects the central row. For non-orthogonal waveforms the obtained linear equalizer can be used to reduce the interference caused by the non-orthogonal waveforms, even if there is no Zero Forcing (ZF) solution. As discussed in [18], [20], linear equalizers might be outperformed by non-linear approaches if PLNC is used. Nonetheless, we will stick to the linear MMSE equalizer (26), as implementation is straightforward. Note, however, that the performance of the non-orthogonal scheme might be improved further, if non-linear equalizers are applied.

IV. Evaluation Metrics

Within this paper, the application of non-orthogonal waveforms is proposed to improve the robustness of PLNC transmission schemes to CFOs and TOs. To show the improvement, compared to classical CP-OFDM schemes, an appropriate evaluation metric is required.

A. SINR

One possible metric is the Signal to Interference and Noise Ratio (SINR). In general, the received signal can be divided into the three components, the desired signal parts of users A and B

$$y_{\mathrm{S,A}}^{(k',\ell')} = \vartheta_{\mathrm{Eq,A}}^{(k,\ell,k',\ell')} d_{\mathrm{A}}^{(k',\ell')} \quad \text{with } (k,\ell) = (k',\ell') \ , \tag{27}$$

the interference terms of users A and B

$$y_{\mathrm{I,A}}^{(k',\ell')} = \sum_{\substack{k \\ (k,\ell)\neq(k',\ell')}} \sum_{\ell} \vartheta_{\mathrm{Eq,A}}^{(k,\ell,k',\ell')} d_{\mathrm{A}}^{(k,\ell)} \tag{28}$$

and a noise term.

With above definitions we can define an SINR of the PLNC system

$$\mathrm{SINR}^{(k',\ell')} = \frac{P_{\mathrm{S,A}}^{(k',\ell')} + P_{\mathrm{S,B}}^{(k',\ell')}}{P_{\mathrm{I,A}}^{(k',\ell')} + P_{\mathrm{I,B}}^{(k',\ell')} + P_{\mathrm{W}}^{(k',\ell')}} \quad . \tag{29}$$

where

$$\begin{aligned} P_{\mathrm{S,A}}^{(k',\ell')} &= \mathrm{E}\left\{ \left| y_{\mathrm{S,A}}^{(k',\ell')} \right|^2 \right\} \\ &= \sigma_S^2 \left| \vartheta_{\mathrm{Eq,A}}^{(k,\ell,k',\ell')} \right|^2 \quad \text{for } (k,\ell) = (k',\ell') \end{aligned} \tag{30}$$

$$\begin{aligned} P_{\mathrm{I,A}}^{(k',\ell')} &= \mathrm{E}\left\{ \left| y_{\mathrm{I,A}}^{(k',\ell')} \right|^2 \right\} \\ &= \sigma_S^2 \sum_{\substack{k \\ (k,\ell)\neq(k',\ell')}} \sum_{\ell} \left| \vartheta_{\mathrm{Eq,A}}^{(k,\ell,k',\ell')} \right|^2 \end{aligned} \tag{31}$$

$$P_{\mathrm{W}}^{(k',\ell')} = \sigma_W^2 \sum_k \sum_\ell \left| z^{(k,\ell,k',\ell')} \right|^2 \int_{-\infty}^{+\infty} g_{\mathrm{Rx}}^2(\lambda) \, d\lambda \, . \tag{32}$$

Parameter σ_S^2 denotes the transmit power and σ_W^2 is the noise power at the relay assuming uncorrelated noise samples.

SINR (29) is an intuitive measure to illustrate the relation of the received signal, interference and noise powers in the MAC phase of the PLNC system. Note, however, that there are some drawbacks. First, it is not necessarily meaningful in the PLNC context. Two users with average link quality can lead to the same SINR values as two users with one good and one bad link. The overall performance of the PLNC system, however, can differ

significantly for these two cases. Secondly, the SINR does not consider the spectral efficiency of the system.

B. Mutual Information

As the SINR is not necessarily meaningful in the MAC phase of the PLNC scheme, we will also compute the mutual information of a PLNC system with GFDM to evaluate the system performance. Without loss of generality, it is assumed that lattice $(k', \ell') = (0, 0)$ is considered at the receiver. In the following illustrations the superscripts $(0, 0)$ will be omitted for the sake of simplicity.

In [19], [21] different decoding and detection schemes for PLNC are analyzed. Especially, the detection scheme in higher Galois Fields called Generalized Joint Channel decoding and Network Coding (G-JCNC) exploits the maximum mutual information for discrete input alphabets of cardinality M and the received superposition, which is based on estimating the relay codeword, directly. Here, the mutual information between the tuple $d_{\mathrm{AB}} = (d_{\mathrm{A}}, d_{\mathrm{B}})$ of cardinality M^2 and the received superposition at the relay is given by [21]

$$I'\left(d_{\mathrm{AB}}; y_{\mathrm{R}}\right) = \sum_{d_{\mathrm{AB}}} \int p\left(y_{\mathrm{R}} \mid d_{\mathrm{AB}}\right) \Pr\left(d_{\mathrm{AB}}\right) \cdot \log_2 \left(\frac{p\left(y_{\mathrm{R}} \mid d_{\mathrm{AB}}\right)}{\sum\limits_{\tilde{d}_{\mathrm{AB}}} \left(p\left(y_{\mathrm{R}} \mid \tilde{d}_{\mathrm{AB}}\right) \Pr\left(\tilde{d}_{\mathrm{AB}}\right)\right)} \right) dy_{\mathrm{R}} \quad (33)$$

where equal a-priori probabilities $\Pr\left(d_{\mathrm{A}}\right) = \Pr\left(d_{\mathrm{B}}\right) = \frac{1}{M}$ are assumed at the sources so that $\Pr\left(d_{\mathrm{AB}}\right) = \frac{1}{M^2}$. Mutual information $I'\left(d_{\mathrm{AB}}; y_{\mathrm{R}}\right)$ corresponds to the maximum sum-rate in the MAC phase of the PLNC scheme. In order to recover the individual messages successfully, the code rate of users A and B has to be smaller than $I = \frac{I'(d_{\mathrm{AB}}; y_{\mathrm{R}})}{2}$ [19]. For $d_{\mathrm{AB}} = (d_{\mathrm{A}}, d_{\mathrm{B}})$, the PDF of the received symbol can be approximated by

$$p\left(y_{\mathrm{R}} \mid d_{\mathrm{AB}}\right) \approx \frac{1}{\pi\left(\sigma_W^2 + \sigma_I^2\right)} e^{-\frac{\left\| y_{\mathrm{R}} - \vartheta_{\mathrm{A}}^{(\mathrm{S})} d_{\mathrm{A}} - \vartheta_{\mathrm{B}}^{(\mathrm{S})} d_{\mathrm{B}} \right\|^2}{\sigma_W^2 + \sigma_I^2}} \quad (34)$$

This approximation assumes that interference is normal distributed. Note that the interference in the considered system is not necessarily normal distributed. However, the PDF of the interference is given by a convolution of the PDFs of the individual interference terms from all neighboring lattice points. According to the central limit theorem, such a PDF tends towards a normal distribution, if many terms are accumulated. For low Signal to Noise Ratios (SNRs), the approximation is also tight as the noise power is much larger than the interference power.

V. Results

Within this section, the robustness with respect to CFOs and TOs will be analyzed for the MAC phase of a PLNC system with orthogonal and non-orthogonal waveforms.

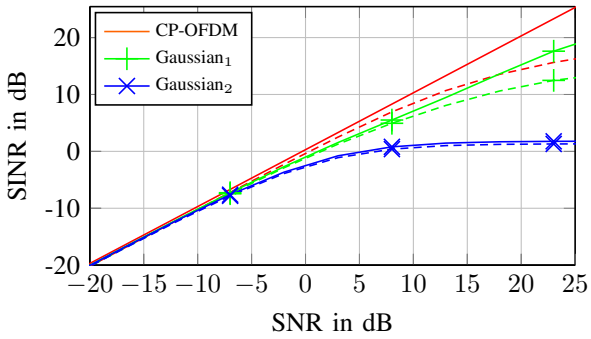

Fig. 6: Average SINR without CFOs ($\Delta\nu_{\max} = 0$, solid) and with CFOs ($\Delta\nu_{\max} = 0.2\,F$, dashed).

The interference caused by the non-orthogonal waveform is treated by the linear MMSE equalizer. In case of the CP-OFDM system, no equalizer is used at the relay node.

A. Simulation Parameters

The SINR, as well as the mutual information, will be analyzed for a rectangular waveform with guard interval (CP-OFDM), and a Gaussian transmit filter with subsequent MMSE equalizer. For the non-orthogonal Gaussian waveform two different modifications Gaussian$_1$ and Gaussian$_2$ will be compared. For Gaussian$_1$, the distance of Gaussian lattice points is chosen such that the spectral efficiency is the same as for CP-OFDM. For Gaussian$_2$, the distance between the Gaussian lattice points is reduced by 25% in each direction to increase spectral efficiency at the cost of additional interference. For both non-orthogonal setups, the localization parameter $\alpha = F^2$ was chosen such that the interference to adjacent lattice points in time domain is the same as the interference to adjacent lattice points in frequency domain.

If synchronization offsets occur in time or frequency, the receiver will no longer match the perfect sampling point, additional interference occurs, and the system performance degrades. For simulation we assume that the synchronization offsets are uniformly distributed random variables in the interval $[-\Delta\nu_{\max}, \Delta\nu_{\max}]$, and $[-\Delta\tau_{\max}, \Delta\tau_{\max}]$, respectively. Furthermore, the offsets of both users are assumed to be independent and the relay is unaware of the synchronization offsets. As the relay is unaware of the offsets, the MMSE equalizer of the non-orthogonal system is designed for the synchronized case $\Delta\nu = 0$, $\Delta\tau = 0$. The interference caused by the synchronization offsets is ignored in the orthogonal and non-orthogonal systems.

Tab. I summarizes the specific simulation parameters for the considered waveforms.

B. SINR

Fig. 6 depicts the SINR of the TWRC at the equalizer output over SNR $2\sigma_S^2/\sigma_W^2$. The solid lines correspond

TABLE I: Applied simulation parameter.

Parameter		CP-OFDM	Gaussian$_1$	Gaussian$_2$
modulation scheme		BPSK		
channel		AWGN		
considered interference terms from neighboring lattice points	N_d	441 ($=21\times21$)		
lattice spacing in frequency domain	F	15kHz	15.52kHz	11.64kHz
lattice spacing in time domain	T	71.4μs	68.97μs	51.73μs
guard interval	T_G	4.7μs $\approx$ 6.5%	–	
number of equalizer coefficients	N_y	–	25 ($=5\times5$)	
normalized distortion parameter of Gaussian waveform	α/F^2	–	1	

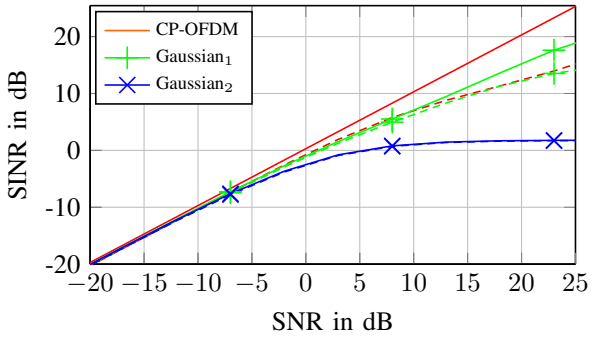

Fig. 7: Average SINR without TOs ($\Delta\tau_\mathrm{max}=0$, solid) and with TOs ($\Delta\tau_\mathrm{max}=0.2\,T$, dashed).

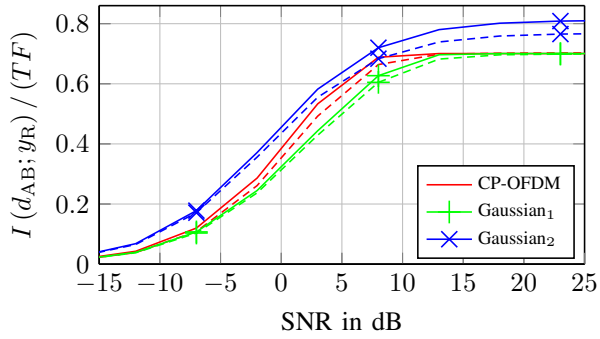

Fig. 8: Normalized mutual information without CFOs ($\Delta\nu_\mathrm{max}=0$, solid) and with CFOs ($\Delta\nu_\mathrm{max}=0.2\,F$, dashed).

to perfectly synchronized systems. As there is no interference in the synchronized orthogonal system, CP-OFDM performs best with SINR = SNR. Contrary, the SINR of non-orthogonal systems is interference limited in the high SNR region. As the interference becomes larger for smaller lattice spacings, Gaussian$_2$ is worse than Gaussian$_1$. For low SNRs, the non-orthogonal waveforms reach the performance of the orthogonal scheme as the noise is much larger than the interference terms.

The dashed lines correspond to the average SINR if the CFOs do not exceed $\Delta\nu_\mathrm{max}=0.2\,F$. As expected, the Gaussian waveform behaves more robust with respect to CFOs. The loss of the non-orthogonal waveforms is smaller than the loss of CP-OFDM. Nonetheless, even Gaussian$_1$ is outperformed by the CP-OFDM scheme at the high SNR region for $\Delta\nu_\mathrm{max}=0.2\,F$, as the residual interference at the output of the MMSE equalizer is worse than the additional interference caused by the CFOs.

Fig. 7 visualizes average SINR results for $\Delta\tau_\mathrm{max}=0.2\,T$. Compared to Fig. 6, the SINR values of the non-orthogonal waveforms do not change, as the Gaussian waveforms have the same shape in time and frequency. For CP-OFDM, however, the influence of CFOs and TOs is different. If the TO can be compensated by the guard interval, the SINR does not change at all, i.e., SINR = SNR again. If the guard interval is not sufficient, severe ISI will be generated and the SINR goes down. Note that both cases might occur for $\Delta\tau_\mathrm{max}=0.2\,T$.

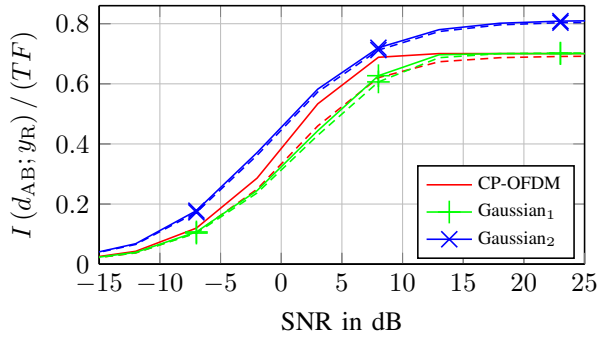

Fig. 9: Normalized mutual information without TOs ($\Delta\tau_\mathrm{max}=0$, solid) and with TOs ($\Delta\tau_\mathrm{max}=0.2\,T$, dashed).

C. Mutual Information

As mentioned above, the SINR results need to be interpreted carefully as the SINR might not be a good performance metric for the PLNC system. Thus, the achievable mutual information (33) will be considered next. The influence of CFOs is shown in Fig. 8, and Fig. 9 visualizes the impact of TOs. Note that the mutual information has been normalized according to the distances of the lattice points.

In terms of mutual information, the Gaussian waveforms can be superior in the PLNC system. For Gaussian$_1$, the increased complexity of the non-orthogonal scheme might not necessarily pay off, as too much residual

interference is left at the output of the linear equalizer. Contrary, Gaussian$_2$ outperforms the other schemes due to the increased spectral efficiency.

The performance gain of the Gaussian waveform can be improved further, if larger synchronization offsets $\Delta\nu_{\max} > 0.2\,T$ are assumed. In that case, however, it might be much more reasonable to spend some more effort to improve the synchronization process.

Reducing lattice distances further will not improve the system performance much. Even if this increases spectral efficiency further, the amount of introduced interference increases considerably. The significant interference is no longer limited to adjacent lattice points and the linear equalizer is no longer able to handle it. Increasing parameter N_{y} of the equalizer will only help to a certain extent, as there is no ZF solution for the PLNC case. Here, non-linear equalizers [22], [23] might be able to improve the PLNC system with non-orthogonal waveforms further.

VI. Conclusion

In this paper the sensitivity of a Physical-Layer Network Coding scheme to synchronization offsets has been investigated for Generalized FDM systems. The system model of the Generalized FDM system has been recapitulated and extended for the PLNC system. Afterwards a matrix notation was introduced to determine a linear MMSE equalizer for the interference caused by neighboring lattice points. Finally, numerical results have been presented, which indicate that the combination of Gaussian waveform and linear MMSE equalizer can outperform classical CP-OFDM systems in PLNC schemes.

VII. Acknowledgment

This work was supported in part by the German Research Foundation (DFG) under grant KU 1221/18-1 and WU 499/10-1 within the priority program "Communication in Interference Limited Networks (COIN)", SPP 1397.

References

[1] S. Zhang, S.C. Liew, and P.P. Lam, "Hot Topic: Physical-layer Network Coding," in *MobiCom 06*, Los Angeles, CA, USA, 2006.

[2] P. Popovski and H. Yomo, "Physical Network Coding in Two-Way Wireless Relay Channels," in *IEEE International Conference on Communications (ICC 07)*, Glasgow, Great Britain, 2007.

[3] C. K. Ho, R. Zhang, and Y.-C. Liang, "Two-Way Relaying over OFDM: Optimized Tone Permutation and Power Allocation," in *2008 IEEE International Conference on Communications*. 2008, IEEE.

[4] K. Jitvanichphaibool, Rui Zhang, and Ying-Chang Liang, "Optimal Resource Allocation for Two-Way Relay-Assisted OFDMA," in *IEEE Global Telecommunications Conference (GLOBECOM 2008)*, New Orleans, LO, 2008.

[5] Fu-nian Li, Guang-xi Zhu, and De-sheng Wang, "Optimal Power Allocation for Two-Way Relaying over OFDM using Physical-Layer Network Coding," *The Journal of China Universities of Posts and Telecommunications*, vol. 18, no. 1, 2011.

[6] H. Shin and J. Lee, "Joint Resource Allocation for Multiuser Two-Way OFDMA Relay Networks with Proportional Fairness," in *IEEE Vehicular Technology Conference (VTC Fall 2011)*, San Francisco, USA, 2011.

[7] B. Han, W. Wang, and M. Peng, "Optimal Resource Allocation for Network Coding in Multiple Two-Way Relay OFDM Systems," in *IEEE Wireless Communications and Networking Conference (WCNC 12)*, Paris, France, 2012.

[8] B. Farhang-Boroujeny, "Ofdm versus filter bank multicarrier," vol. 28, no. 3, May 2011.

[9] V. Vakilian, T. Wild, F. Schaich, and S. ten Brink, "Universal-Filtered Multi-Carrier Technique for Wireless Systems Beyond LTE," in *GLOBECOM 2013 - 2013 IEEE Global Telecommunications Conference*, Atlanta, GA, USA, 2013.

[10] J. Du, *Pulse Shape Adaptation and Channel Estimation in Generalised Frequency Division Multiplexing Systems*, Licentiate thesis in electronics and computer systems, KTH, Stockholm, Sweden, November 2008.

[11] G. Fettweis, M. Krondorf, and S. Bittner, "GFDM - Generalized Frequency Division Multiplexing," in *Vehicular Technology Conference, VTC Spring 2009. IEEE 69th*, Barcelona, Spain, April.

[12] G. Wunder, P. Jung, M. Kasparick, T. Wild, F. Schaich, Y. Chen, S. ten Brink, I. Gaspar, N. Michailow, A. Festag, L. Mendes, N. Cassiau, D. Ktï¿½nas, M. Dryjanski, S. Pietrzyk, B. Eged, P. Vago, and F. Wiedmann, "5GNOW: Non-Orthogonal, Asynchronous Waveforms for Future Mobile Applications," *Communications Magazine, IEEE*, vol. 52, no. 2, February 2014.

[13] W. Kozek and A.F. Molisch, "Nonorthogonal Pulseshapes for Multicarrier Communications in Doubly Dispersive Channels," *IEEE Journal on Selected Areas in Communications*, vol. 16, no. 8, Oct 1998.

[14] A. Sahin, I. Guvenc, and H. Arslan, "A Survey on Multicarrier Communications: Prototype Filters, Lattice Structures, and Implementation Aspects," *Communications Surveys Tutorials, IEEE*, vol. PP, no. 99, 2013.

[15] M. Wu, F. Ludwig, M. Woltering, D. Wübben, A. Dekorsy, and S. Paul, "Analysis and Implementation for Physical-Layer Network Coding with Carrier Frequency Offset," in *International ITG Workshop on Smart Antennas (WSA2014)*, Erlangen, Germany, Mar 2014.

[16] D. Wübben, "Joint Channel Decoding and Physical-Layer Network Coding in Two-Way QPSK Relay Systems by a Generalized Sum-Product Algorithm," in *Communication Systems (ISWCS), 2010 7th*, York, Great Britain, Sept. 2010.

[17] D. Wübben and Y. Lang, "Generalized Sum-Product Algorithm for Joint Channel Decoding and Physical-Layer Network Coding in Two-Way Relay Systems," in *2010 IEEE Global Telecommunications Conference GLOBECOM 2010*, Miami, Fl, USA, Dec. 2010, IEEE.

[18] A. Schmidt, W. Gerstacker, and R. Schober, "Maximum SNR Transmit Filtering for Linear Equalization in Physical Layer Network Coding," in *Globecom Workshops (GC Wkshps), 2012 IEEE*, Dec 2012.

[19] M. Wu, D. Wübben, and A. Dekorsy, "Mutual information based analysis for physical-layer network coding with optimal phase control," in *Conference on Systems, Communication and Coding (SCC), Proceedings of 2013 9th International ITG*, Jan 2013.

[20] U. Bhat and T.M. Duman, "Decoding Strategies for Physical-Layer Network Coding over Frequency Selective Channels," in *Wireless Communications and Networking Conference (WCNC), 2012 IEEE*, April 2012.

[21] S. Pfletschinger, "A Practical Physical-Layer Network Coding Scheme for the Uplink of the Two-Way Relay Channel," in *Conference Record of the Forty Fifth Asilomar Conference on Signals, Systems and Computers (ASILOMAR)*, 2011.

[22] K. Matheus, K. Knoche, M. Feuersanger, and K. D Kammeyer, "Two-dimensional (recursive) Channel Equalization for Multicarrier Systems with Soft Impulse Shaping (MCSIS)," in *Global Telecommunications Conference, 1998. GLOBECOM 1998. The Bridge to Global Integration. IEEE*, 1998, vol. 2.

[23] A. Schmidt, W. Gerstacker, and R. Schober, "Maximum SNR Transmit Filtering for Decision-Feedback Equalization in Physical Layer Network Coding," in *Conference on Systems, Communication and Coding (SCC), Proceedings of 2013 9th International ITG*, Jan 2013.